Scalability of Quantum Simulations of Thermoelectric Superlattice Devices

T.D. Musho[a], D.G. Walker[b]

[a]*Interdisciplinary Materials Science, Vanderbilt University, Nashville, Tennessee 37212, USA*
[b]*Department of Mechanical Engineering, Vanderbilt University, Nashville, Tennessee 37212, USA*

Abstract

The effects of layer thickness and periodicity on thermoelectric properties of Si/Ge superlattice materials are studied through a non-equilibrium Green's function (NEGF) computational approach. Results show an independence of Seebeck coefficient for increasing the number of superlattice periods. Additionally, a critical layer thickness is obtainable to achieve a favorable transmission spectrum while maximizing hetero-interface density. These findings are important to researchers who computationally explore thermoelectric properties of nanostructured materials. In particular, these results identify ranges of parameters worthy of further experimental study.

Introduction

Short period Si/Ge superlattice thermoelectric materials are interesting primarily because they exhibit reduced thermal conductivity compared to the bulk phases of the layer constituents [1]. Consequently the thermoelectric figure of merit for these materials has been improved experimentally [1]. Theoretical investigation of these structures has relied heavily on molecular dynamics or Boltzmann transport models for thermal transport studies. The electrical side of the problem has received much less attention because researchers often assume that the electrical modifications due to interface scattering are less significant due to the disparity of mean free paths between electrons and phonons [2]. This assumption is simply not true, and Bulusu et. al [3] were one of the first groups

*Corresponding author
Email address: greg.walker@vanderbilt.edu (D.G. Walker)

to examine the question computationally. The Green's function approach used in that study solved the Schrödinger-Poisson system under thermal and electrical bias to estimate the power factor ($S^2\sigma$), where S is the Seebeck coefficient and σ is the electrical conductivity, for layered structures. The Green's function approach allows a bias to be added to the system at the contact making it a non-equilibrium approach. Their work, though, considered a three-layer system, which, we contend, does not fully capture the repetitive nature of the barrier/well structure.

Previous non-equilibrium Green's function (NEGF) research [4] in the area of electrical transport as it relates to thermoelectric properties has focused on single bilayer nanostructures, in which a select material is sandwiched between a dissimilar material forming two heterojunctions. The heterojunction forms a contact/barrier/well/barrier/contact structure. To a first order approximation, the performance of these single bilayer devices matches—at least in terms of trends—the actual devices because the barrier/well structure is responsible for the transport in the simulation as well as in an actual device. However, the effects of the contact can dominate the behavior of the simulated device because the device is so small [5]. Moreover, a single bilayer (one well surrounded by two barriers), is not likely to provide an accurate representation of a periodic structure. Therefore previous simulations of devices with reduced number of layers can be dubious. In defense of the past efforts, the problem can be quite computationally intensive and modern facilities are only now making physically realistic solutions accessible.

This research extends those initial NEGF studies to determine how well a reduced system can model a larger structure with repeating elements. When attempting to compute material properties for structure that repeats over a long range, we need to insure that the influence of the contacts are negligible and that the long-range effects are captured in the model. The effects of layer thickness and number of periods on electrical properties are examined through a non-equilibrium Green's function (NEGF) computational approach. This work answers the question of whether a small number of layers can be used to simulate

the behavior of a many-layer device, and whether an optimal superlattice layer thickness will maximize electrical transport properties.

Coincidentally, the same effects can be seen when calculating thermal conductivity in superlattices, which is a complementary line of study in nanostructured thermoelectrics. Many researchers [6, 7] have exploited increased interface density of superlattices to reduce the phonon thermal conductivity. Zhang [8] showed that the simulated thermal conductance decreases with number of layers but converges at layer thicknesses above five unit cells or about 1.3 nm. Furthermore, the thermal resistance becomes independent of number of interfaces between eight and ten Si/Ge interfaces or four and five bilayers. This means that the thermal performance of a material with hundreds of periods can be effectively modeled using a system of only a handful of layers.

The computational method employed to calculate the electrical transport properties is a self-consistent Schrödinger-Poisson type solver. A non-equilibrium Green's function (NEGF) computational method [9] was implemented to solve the one-dimension wave equation (see Equation 6). This model has been used in previous research [4] to study the electrical transport in superlattice thermoelectric structures with good agreement given the available experimental data. The self-consistency arises from determining a solution that satisfies both the wavefunctions calculated from Schrödinger equation and the potential field described by Poisson's equation.

By solving the wavefunction and the potential solutions self-consistently any variation including band bending or confinement can be readily captured. The conduction band edge of the unperturbed Hamiltonian is assumed constant throughout the layer thickness and is determined based on the effective mass description. The effective conduction band edge is determined from the bulk value, which is adjusted to incorporate doping [3] and strain [4]. Because the thickness of the layers is quite small, the constant-band approximation is acceptable. Therefore, the resulting band description of the SL material forms a rectangular potential well structure, illustrated in Figure 1. A review on the technique compared to other thermoelectric models is provided by Bulusu [10].

The only modification of the code from previous simulations was incorporation of an Anderson mixing technique [11] to increase the rate of convergence of Poisson's equation. This method relies on five previous iterative solutions and the latest calculated charge distribution to forecast a new solution based on the weight average of these previous values. The Anderson mixing technique proves to be a major computational speed-up compared to a simple mixing technique which only relies on the most recent potential solution. Even though the inversion of the Green's function is the most computational expensive function, the updated algorithm afforded significant gains of up to an order of magnitude in computational speed.

In this NEGF formalism we are only interested in the conduction electrons within a range of energy from the lowest conduction band edge up to $3k_BT$ above the largest barrier height. Following Datta's [9] explanation, the domain is discretized such that the wavefunctions within each discretized cell can fully capture the energy range of interest. A grid study was carried out in order to determine the required domain discretization and energy range discretization. A discretized cell size of 0.5 Å was used and 5200 energy integration points were required between a energy range of -0.2 eV and 1 eV.

To computationally determine the Seebeck coefficient of a superlattice material, a temperature difference is applied to the contacts, which induces a current in the device. Next, an external potential is applied at the contacts opposing the current. The Seebeck voltage is defined as the voltage that results in zero current through the device and is a function of the temperature difference across the device. In essence, the thermally induced current opposes the voltage-induced current. The Seebeck coefficient is obtained by normalizing the Seebeck voltage by the temperature difference and is a function of the average temperature of the device, not the temperature difference across the device. The slope of the IV curve is the electrical conductance. Between these two parameters—Seebeck coefficient (S) and electrical conductivity (σ)—the power factor can be obtained as a product (PF=$S^2\sigma$).

The superlattice materials in the present study are [001] isotropic silicon

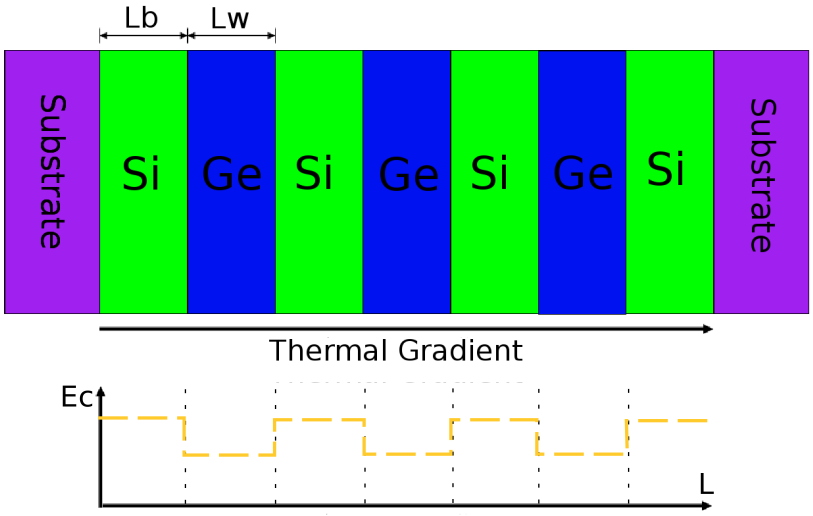

Figure 1: Sketch of a superlattice device with three bilayers and a silicon cap. A 10K thermal gradient is applied in the cross-plane direction. The strained conduction band edge which forms the rectangular well structure is illustrated below. The device is doped with $10^{18}\,\mathrm{cm}^{-3}$ electrons. Substrate effects are neglected in all results.

and germanium described by an effective mass Hamiltonian. The contacts are assumed to be ohmic in nature with self-scattering properties [12]. The spacial geometry of the superlattice structure has a finite extent in the transport direction (cross-plane) and an infinite extent in the other directions (in-plane). In the forgoing research, silicon will always neighbor the ohmic contacts (see Figure 1). The dopant concentration is maintained at $10^{18}\,\mathrm{cm}^{-3}$ for all cases. Transport is ballistic in nature and scattered only at the contacts.

Straining of the layers was taken into account and becomes a important effect due to the modification of the band structure [13]. The offset of the conduction band edge in both bilayer materials is calculated by a weighted average of layer thickness, lattice constants and deformation potentials [14]. The expression used to calculate the offset first requires the calculation of effective lattice parameters

parallel and perpendicular to the strain tensor,

$$a_{||} = \frac{a_1 G_1 h_1 + a_2 G_2 h_2}{G_1 h_1 + G_2 h_2} \tag{1}$$

$$a_{\perp} = a_1[1 - D_i(a_{||}/a_n - 1)] \tag{2}$$

In Equation 1, a_n is the lattice constant of the material, G_n is the shear modulus, and h_n is the individual layer thickness of each constitute bilayer material. The shear modulus, $G_n^{001} = 2(c_{11} + 2c_{12})(1 - c_{12}/c_{11})$, is a function of the elastic constants, c_{11} and c_{12}. Next, the calculated effective lattice constant $(a_{||}, a_{\perp})$ can be used to determine the in-plane strain tensor based on the ratio of the effective lattice constant to the actual lattice constant(a_n).

$$\epsilon_{n||} = \frac{a_{||}}{a_n} - 1; \tag{3}$$

$$\epsilon_{n\perp} = \frac{a_{\perp}}{a_n} - 1. \tag{4}$$

The expression for the conduction band offset is given as

$$\Delta E_c^{001} = \frac{2}{3}\Xi(\epsilon_{\perp} - \epsilon_{||}), \tag{5}$$

where Ξ is the tabulated deformation potential in Table 2 of reference [14]. The deformation potential is selected for both the silicon and germanium material in the [001] crystallographic direction.

Because the structure is infinite in extent for both transverse directions the Hamiltonian is expressed as a 1D Hamiltonian with units of energy per unit length squared. Thus, the effective mass description takes the following form

$$H\psi = \frac{-\hbar^2}{2m^*}\left(\frac{\partial^2}{\partial x^2}\right)\psi = \epsilon_n \psi_n. \tag{6}$$

This expression is implemented to calculate both the steady state eigenvalues of the unperturbed system and ultimately to construct the Green's function and determine the transmission.

The transmission, as described by Datta [9], is the product of the advancing and retarding Green's function multiplied from the source and drain broadening term. One can conceptualize this as the probability that a single electron will

Authors	Layer Size [nm]	Periods	Seebeck [μV/K] Experimental	Numerical
Koga [15]	Si(2)/Ge(2)	100	220	159
Yang [1]	Si(7.5)/Ge(1.5)	110	300	230
Yang [16]	Si(0.5)/Ge(0.7)	100	500	352

Table 1: Comparison of NEGF results to experimental results by other researchers. NEGF results were calculated using four layers.

transport across the device at a given energy level. The net current across the device is determined by the Landauer formula in which summation of the transmission at discrete energy levels is multiplied times the quantum conductance and the Fermi-Dirac distribution at each contact.

The NEGF code was validated by comparing Seebeck coefficients of known experimental devices from the literature. Table 1 outlines the comparison for a device with four periods, and agreement is reasonable given our effective mass description and uncertainties in experimental parameters.

In Figure 2 with four different layer thicknesses, the number of bilayers is increased to examine the convergence of the simulations to a constant value, which represents a large number of pairs. The layer thickness increases the Seebeck coefficient to a plateau around 1400 μV/K. This effect is contrary to Hicks [2], who suggested that low dimensional materials would exhibit enhanced local density of states at the Fermi level. While this hypothesis is correct, the proximity of the levels relative to the conduction band is also important in practice. At individual layer thickness above 3nm the asymptotic behavior in the Seebeck coefficient in Figure 2(a) is attributed to the shape of the transmission spectrum. O'Dwyer [17] eludes to a localization of transmission in his research and points to the increased efficiency for sharp transmission but does not carry out the calculation to determine the limiting layer thickness. By varying the layer thickness in a simple bilayer device (see Figure 3), the transmission changes significantly between a device with a 1nm individual layer thickness compared to a device with a 4nm individual layer thickness. However, the thermoelectric performance difference between the 3 nm and 4 nm device is considerably less

significant. This can be explained because the majority of the electrons that govern the transport lie within k_BT of the conduction band (0.4 eV). Thus, a superlattice material with good thermoelectric properties must exhibit not only a sharp transmission peak but also a peak near the conduction band edge.

As shown in Figure 2(a) the Seebeck coefficient is essentially independent of the number of bilayers with perhaps a slight deviation for structures less than 3 or 4 bilayers. These findings are important because they suggest the Seebeck performance of a device with a periodicity of hundreds bilayers can be modeled with a three layer device. This asymptotic behavior is best understood through examination of the trends in the transmission spectrum. Figure 4 shows the transmission for two structures—(a) a 1 bilayer system and a (b) 5 bilayer system. From the 5 bilayer device [Figure 4(b)], narrow peaks in the transmission at an energy below the barrier conduction band edge of 0.4 eV are apparent. These narrow transmission peaks below the conduction band edge are attributed to tunneling electrons that lie at the conduction band edge of the silicon (electronic well). Studying the eigenvalues (sub-band levels) of the unperturbed Hamiltonian, the tunneling electrons are a function of near degeneracies in the electronic eigenstates around the silicon (electronic well) conduction band edge. An interesting trend of these peaks are that they appear within a range of 0.12 eV to 0.15 eV in quantities of one less than the number of layers. For example, the five bilayer device has four peaks, see inset plots. As the number of layers increase above four layers, more peaks appear, but the range, magnitude and position of the peaks changes very little. Moreover, the broadening tends to wash out any effects that might arise from having sharp discrete peaks. Because the current is related to the integral of the transmission, the change in performance related to adding more peaks with each bilayer is diminishing. Consequently, the convergence in the Seebeck coefficient is attributed to the marginal increase in transmission for devices with periodicity above three layers.

This marginal increase in Seebeck coefficient is evident in Figure 2 from one to approximately three bilayers as a result of the formation of transmission peaks between 0.12 eV to 0.15 eV as seen in the 5 bilayer device. Because the integral

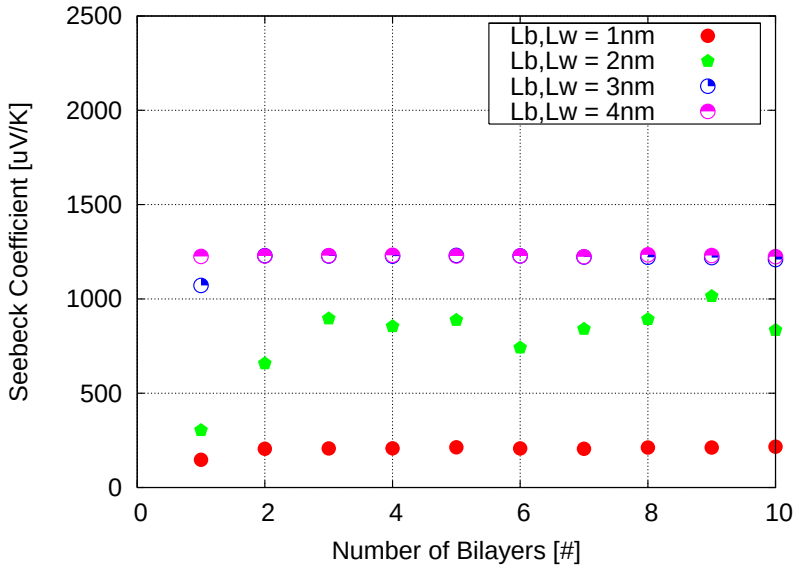

(a)

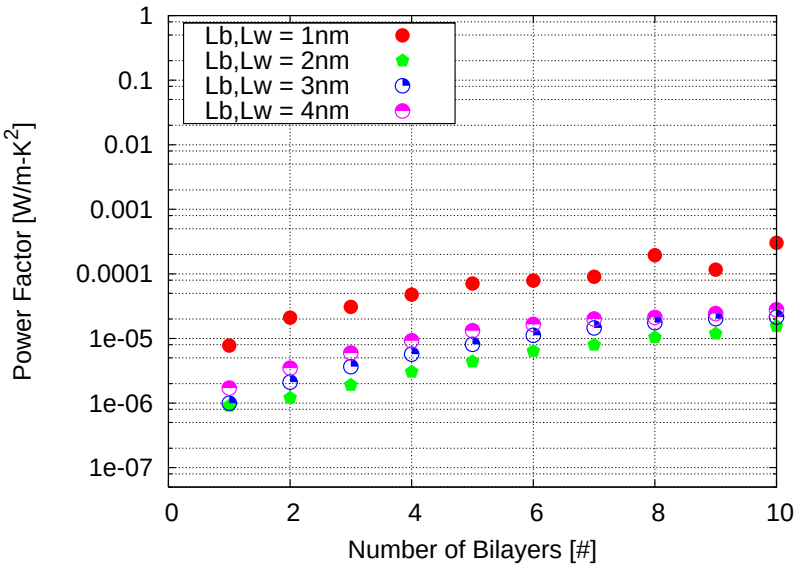

(b)

Figure 2: As the number of layer pairs increase the electrical properties become independent. (a) Seebeck coefficient, (b) power factor.

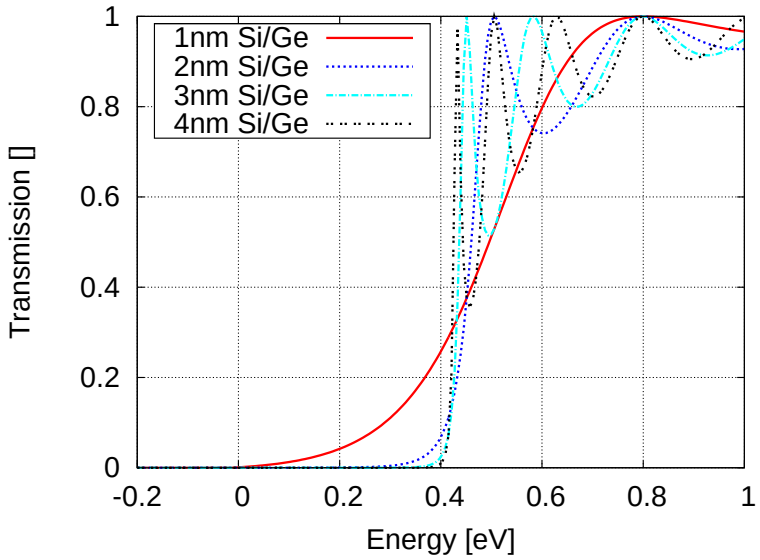

Figure 3: Transmission plot of a Si/Ge thermoelectric with 10K temperature difference. As the individual layer thickness of both the Si and Ge increase the transmission sharpness becomes more pronounced.

transmission between 0.12 eV to 0.15 eV when increasing from two bilayers and greater there is a negligible change in Seebeck coefficient for devices with more than 3 bilayers.

Figure 2(b) of the power factor gives an estimate of the electrical side of the thermoelectric performance; the greatest value is achieved for the 1 nm layer device. However, if we consider Seebeck alone [Figure 2(a)], the largest coefficient is achieved for devices with individual layer thicknesses above 3 nm and more than two bilayers.

The results suggest that the sharpness and location of the transmission spectrum is responsible for identifying a critical layer thickness of 3 nm, which provides an optimal Seebeck coefficient and interface density. Moreover, the number of bilayers required to reach the performance of an "infinite" bilayer system can be reached with relatively few numbers of layers (less than 10), and the Seebeck coefficient requires even fewer (3 to 4). These results are commensurate with

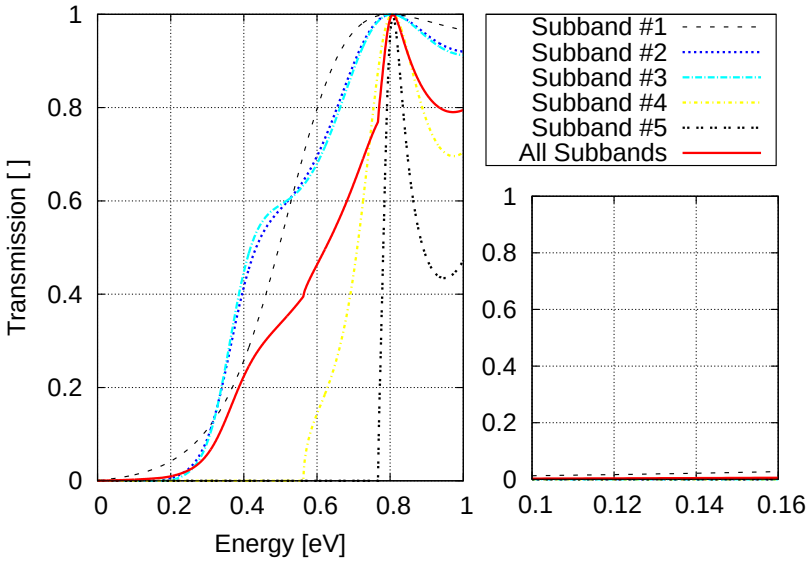

(a)

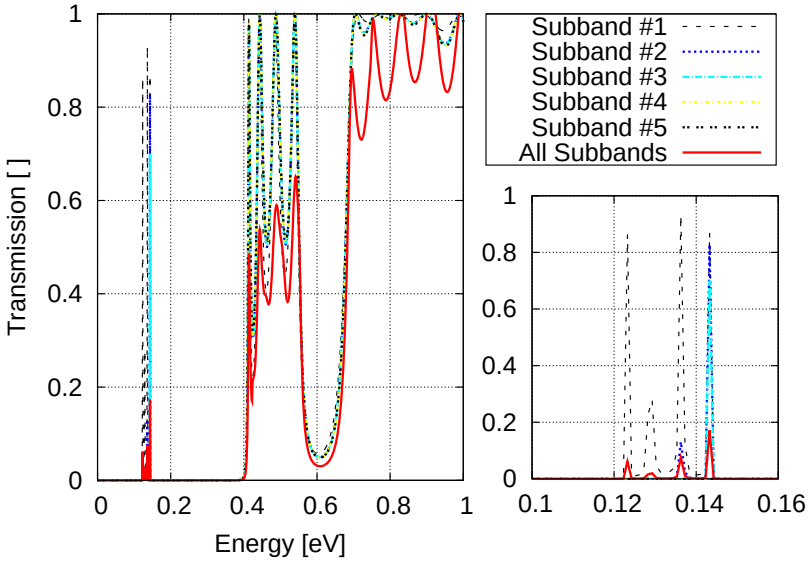

(b)

Figure 4: Transmission for two difference periodicities of a Si(1 nm)/Ge(1 nm) device. (a) 1 bilayers (b) 5 bilayers. Transmission peaks below the conduction band edge (0.4 eV) in (b) are tunneling electrons at silicon conduction band edge.

the findings from Zhang [8] for thermal transport properties meaning that simulations of fully coupled thermoelectric superlattice materials is possible with limited system.

Furthermore, comparison between the numerical results of a 4 bilayer device to experimental devices of hundreds of bilayers validates our findings. Matching the dopant concentration and temperature to the associated experimental setup equivalent numerical devices can be simulated. Table 1 summarizes numerical values and experimental values found in the available literature. The trends and order of magnitude match well (given experimental and fabrication uncertainty) and provide evidence that the NEGF is a valid method of calculating Seebeck coefficient and that 4 bilayers is an adequate simulation device size to determine the overall Seebeck performance of larger experimental SL structures.

The scalability of the code is shown in Figure 5 and corresponds to the wall time required for each device studied. Comparing the wall time of any two devices, we find that the problem scales as N^2. This scaling is not unexpected because the code spends the majority of its time performing matrix inversions, which also scales as N^2. Decomposition and back substitution are not possible since the inverted matrix is used directly to solve an array of linear problems. The wall times are based on running the parallelized code on 20 processors where the energy domain is decomposed across all processors; the results are then reduced to a single processor (one call to `MPI_Reduce`). Because the problem is trivially parallel, the parallel scalability is essentially linear up to the number of processors tested. We expect the scalability to remain linear for large numbers of processors. However, for problems larger than the superlattices tested here, the present strategy will require inordinate amounts of RAM, and a domain decomposition technique may become preferable.

Conclusion

The electron transport properties of a many-layer thermoelectric superlattice device was studied computationally using non-equilibrium Green's function

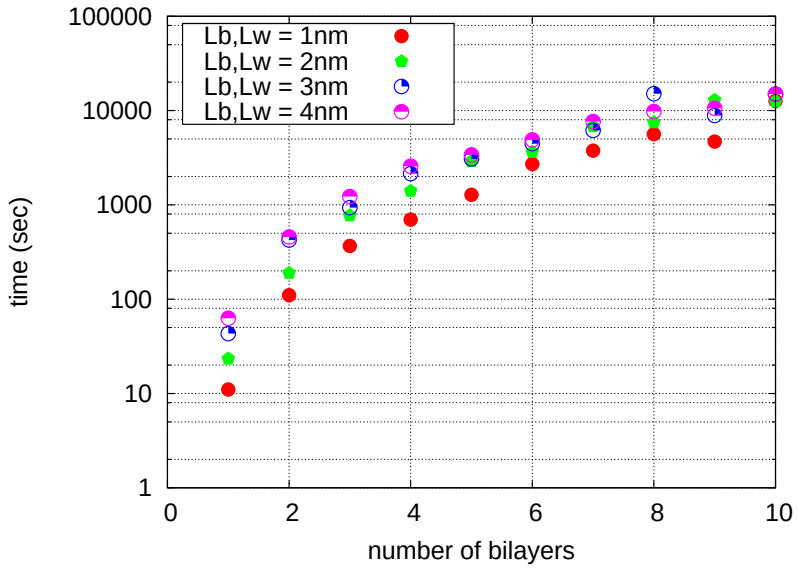

Figure 5: Plot of the wall time as a function of number of bilayers. All devices were run across 20 processors where the energy domain was decomposed across all processes.

(NEGF) method. The NEGF allowed a wave point of view to capture the underlying quantum effects in nanoscale electron transport through a barrier/well structure. Based on the sharpness of the transmission spectrum a critical layer thickness at which an optimal Seebeck coefficient exists and a high interface density was determined to be 3 nm for each independent layer. The study also found that the computed Seebeck coefficient is independent of the number of layers. Although, the electrical conductivity appears to be independent of the number of layers above eight, additional tests may be needed to verify this claim. Nevertheless, we believe a simulated device with eight layers can capture the essence and performance of a many-layer device.

[1] B. Yang, J. L. Liu, K. L. Wang, and G. Chen. Simultaneous measurements of seebeck coefficient and thermal conductivity across superlattice. *Applied Physics Letters*, 80(10):1758–1760, March 2002.

[2] L. D. Hicks and M. S. Dresselhaus. Effect of quantum-well structures on

the thermoelectric figure of merit. *Physical Review B*, 47(19):12727–12731, May 1993.

[3] A. Bulusu and D. G. Walker. Quantum confinement effects on the thermoelectric properties of semiconductor nanofilms and nanowires. *IEEE Transactions on Electron Devices*, 55(1):423–429, January 2008.

[4] A. Bulusu and D. G. Walker. Quantum modeling of thermoelectric performance of strained Si/Ge/Si superlattices using the nonequilibrium green's function method. *Journal of Applied Physics*, 102(7):073713, October 2007.

[5] Haiyan Jiang, Sihong Shao, Wei Cai, and Pingwen Zhang. Boundary treatments in non-equilibrium green's function (NEGF) methods for quantum transport in nano-MOSFETs. *Journal of Computational Physics*, 227(13):6553–6573, 2008.

[6] Y. Chen, D. Li, J. R. Lukes, Z. Ni, and M. Chen. Minumum superlattice thermal conductivity from molecular dynamics. *Physical Review B*, 72(174302):1–6, November 2005.

[7] S. M. Lee, G. Matamis, and D. G. Cahill. Thin-film materials and minimum thermal conductivity. *Microscale Thermophysical Engineering*, 2:31–36, 1998.

[8] W. Zhang, T. S. Fisher, and N. Mingo. The atomistic green's function method: An efficient simulation approach for nanoscale phonon transport. *Numerical Heat Transfer Part B-Fundamentals*, 51(4):333–349, 2007.

[9] S. Datta. *Quantum Transport: Atom to Transistor*. Cambridge University Press, New York, 2005.

[10] A. Bulusu and D. G. Walker. Review of transport modeling for thermoelectric materials. *Superlattices and Microstructures*, 44(1–36), April 2008.

[11] V. Eyert. A comparative study on methods for convergence acceleration of iterative vector sequences. *Journal of Computational Physics*, 124(2):271–285, 1996.

[12] S. Datta. Nanoscale device modeling: the green's function method. *Superlattices and Microstructures*, 28(4):253–278, 2000.

[13] A. Bulusu and D. G. Walker. Modeling of thermoelectric properties of semiconductor thin films with quantum and scattering effects. *Journal of Heat Transfer*, 129(4):492–499, April 2007.

[14] C. G. Van de Walle. Band lineups and deformation potentials in the model-solid theory. *Physical Review B*, 39(3):1871–1883, January 1989.

[15] T. Koga, S. B. Cronin, M. S. Dresselhaus, J. L. Liu, and K. L. Wang. Experimental proof-of-principle investigation of enhanced $Z_{3D}T$ in (001) oriented Si/Ge superlattices. *Applied Physics Letters*, 77(10):1490–1492, sep 2000.

[16] B. Yang, W. L. Liu, J. L. Liu, K. L. Wang, and G. Chen. Measurements of anisotropic thermoelectric properties in superlattices. *Applied Physics Letters*, 81(19):3588–3590, nov 2002.

[17] M. F. O'Dwyer, R. A. Lewis, C. Zhang, and T. E. Humphrey. Electronic efficiency in nanostructured thermionic and thermoelectric devices. *Phys. Rev. B*, 72(20):205330, Nov 2005.